



OPEN

Fractional tunnelling resonance in plasmonic media

SUBJECT AREAS:

SUB-WAVELENGTH
OPTICSNANOPHOTONICS AND
PLASMONICS

METAMATERIALS

MICRORESONATORS

Ji-Hun Kang & Q.-Han Park

Department of Physics, Korea University, Seoul 136–701, Korea.

Received
17 April 2013Accepted
25 July 2013Published
13 August 2013Correspondence and
requests for materials
should be addressed to
Q.-H.P. (qpark@korea.
ac.kr)

Metals can transmit light by tunnelling when they possess skin-depth thickness. Tunnelling can be resonantly enhanced if resonators are added to each side of a metal film, such as additional dielectric layers or periodic structures on a metal surface. Here we show that, even with no additional resonators, tunnelling resonance can arise if the metal film is confined and fractionally thin. In a slit waveguide filled with a negative permittivity metallic slab of thickness L , resonance is shown to arise at fractional thicknesses ($L = \text{Const.}/m$; $m = 1, 2, 3, \dots$) by the excitation of ‘vortex plasmons’. We experimentally demonstrate fractional tunnelling resonance and vortex plasmons using microwave and negative permittivity metamaterials. The measured spectral peaks of the fractional tunnelling resonance and modes of the vortex plasmons agree with theoretical predictions. Fractional tunnelling resonance and vortex plasmons open new perspectives in resonance physics and promise potential applications in nanotechnology.

Resonance is a fundamental property of electromagnetic waves which plays a key role in numerous photonic applications such as optical filters^{1,2}, nanosensors^{3–5}, non-classical light sources^{6,7}, nanolasers^{8–12}, metamaterials^{13,14}, and photovoltaic cells¹⁵. Light transmission through a dielectric slab in a waveguide for instance can be resonantly increased by the constructive interference of multiply reflected waves inside the dielectric slab. Metals, or materials possessing negative permittivity, admit only evanescent waves so that light transmission occurs through tunnelling and resonance is in general suppressed. Similar to the resonant tunnelling of electrons through double potential barriers¹⁶, photon tunnelling can be resonantly enhanced with the help of additional resonance structures such as high-index dielectric layers^{17,18}, periodic structures on a metal surface^{19–21} causing the constructive interference of surface plasmon waves, grating structures for broadband transmission^{22,23} or even a split-ring-resonator²⁴. An immediate question is whether these additional resonance structures are essential for the resonant photon tunnelling. Surprisingly, the answer is no.

Here, we introduce a resonant photon tunnelling with no additional resonance structures, so called fractional tunnelling resonance (FTR), that occurs in a slit waveguide filled with a negative permittivity slab. FTR is a structural resonance in which the slab thickness must be a fractional multiple of a unit thickness, in contrast to the integer multiple thicknesses of Fabry–Perot resonators. We show that FTR arises from vortex plasmons that channel circulating energy flows in the form of optical vortex pairs. To demonstrate FTR experimentally, we conducted microwave measurement of near and far fields by using metamaterial samples of relatively low negative permittivity and little loss. The Drude-type frequency dispersion of the metamaterials allows spectral representation of FTR at a fixed thickness. We measured the spectral peaks of FTR and the resonance modes of vortex plasmons, which agree well with theoretical predictions.

Results

Fractional tunnelling resonance and vortex plasmons. For a better understanding of FTR and vortex plasmons, we consider a waveguide cavity formed by a slit in a perfect electric conductor, as shown in Fig. 1. We investigate the behaviour of light passing through the slit by solving Maxwell’s equation numerically using the finite-difference time-domain (FDTD) method. When filled with a dielectric medium of positive permittivity, the slit in Fig. 1a exhibits Fabry–Perot resonance when the optical path length is roughly an integer multiple of the half-wavelength. If the length L of a slit waveguide is much smaller than a half-wavelength, or if the filling medium has negative permittivity so that light becomes attenuated, one generally expects no resonance in either case. However, the numerical results in Fig. 1b exhibit a surprising occurrence of resonances in a negative permittivity slab of thickness L much smaller than a half-wavelength. Resonances appear at fractional thicknesses $L_m = L_1/m$ ($m = 1, 2, 3, \dots$), where the unit thickness L_1 is much smaller than the wavelength. Numerical results show that the resonance mode indicated by an integer m consists of m pairs of optical vortices of opposite circulation. In

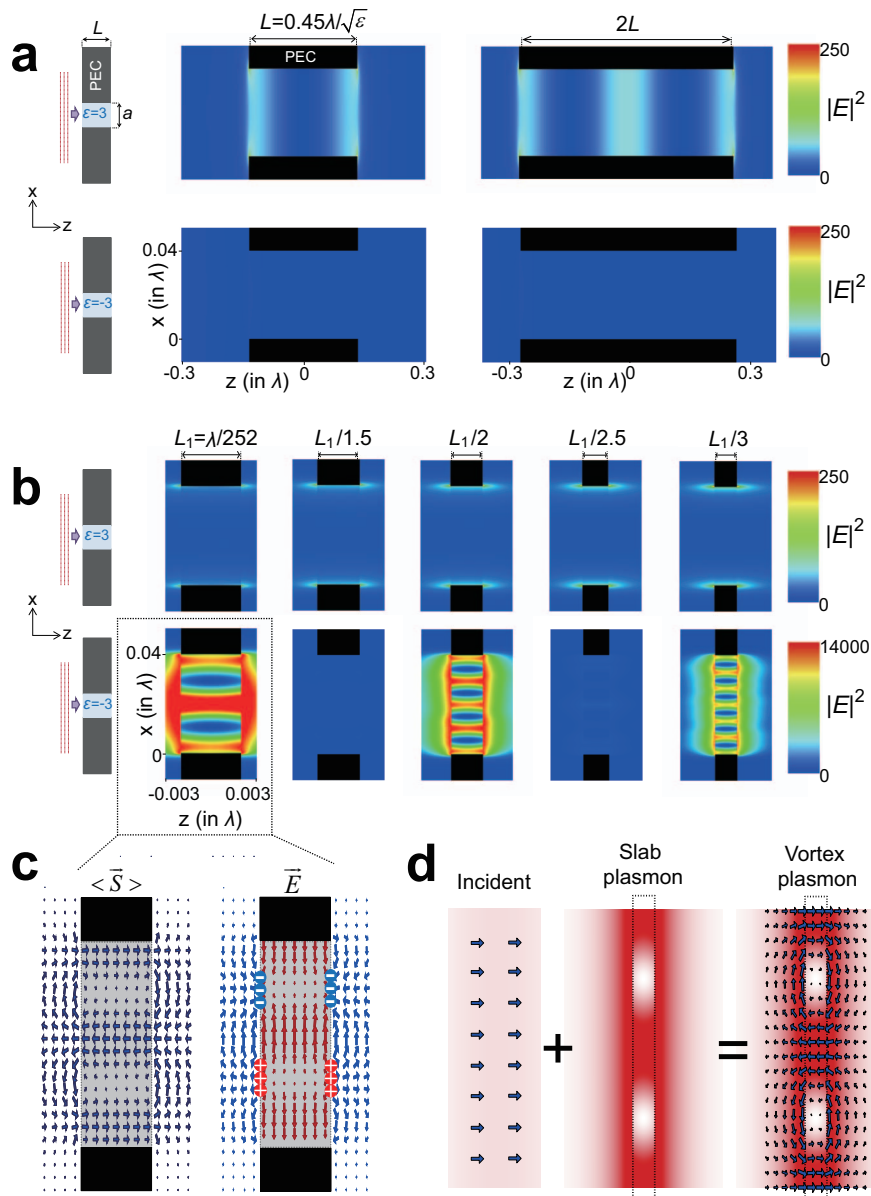


Figure 1 | Fabry-Perot resonance and FTR by a single slit in a perfect electrical conductor. (a) Electric field intensity profiles inside slit waveguides with an incident wave polarized vertically to the slit direction. Slit is filled with either a dielectric material having positive permittivity $\epsilon = 3$ or a metallic material with $\epsilon = -3 + 0.001i$. Slit width a is 0.04λ , where λ is the wavelength. (b) Intensity profiles inside very thin slit waveguides. Resonance arises when the slit is filled with a metallic material of thickness L which is a fraction of the unit thickness L_1 , i.e., $L = (1/m)L_1$ for $m = 1, 2, 3, \dots$ (c) Vector field maps for the $m = 1$ vortex plasmon obtained by FDTD numerical calculation. The time-averaged Poynting vector (left) represents circulating energy flows, whereas electric vectors (right) show localized plasmonic currents and local fields generated by induced charges. (d) Vortex plasmon vs. slab plasmon. Vortex plasmon is a coupled state between an incident plane wave passing through a slab and a slab plasmon. Arrows are time-averaged Poynting vectors; colour maps represent electric field intensities. Slab plasmon has zero time-averaged energy flow.

Fig. 1c, the time-averaged energy flow and electric field profiles obtained by the FDTD method are given explicitly for the $m = 1$ resonance mode. These optical vortices form through highly localized excitation of plasmonic currents and induced charges that guide the electromagnetic energy so that energy flows as paired vortices.

Coupled mode theory for fractional tunnelling resonance. FTR can be predicted analytically by a coupled-mode diffraction theory^{25,26}. When transverse magnetic light is incident normally onto a slit in a perfectly conducting plate of thickness L filled with a negative permittivity medium, we may express the magnetic field in three regions—below (region I), inside (region II), and above (region III) the slit—in the following form with the time harmonic term suppressed,

$$\begin{aligned}
 H_y^{(I)}(x, z) &= \sqrt{\frac{\epsilon_0}{\mu_0}} \int_{-\infty}^{\infty} dk \left[\delta(k) e^{ikx + i\sqrt{k_0^2 - k^2}(z + L/2)} + \right. \\
 &\quad \left. \rho(k) e^{ikx - i\sqrt{k_0^2 - k^2}(z + L/2)} \right], \quad z \leq -\frac{L}{2} \\
 H_y^{(II)}(x, z) &= \sqrt{\frac{\epsilon_0}{\mu_0}} \sum_{m=0}^{\infty} u_m(x) [A_m e^{i\theta_m z} + B_m e^{-i\theta_m z}], \quad (1) \\
 &\quad -\frac{L}{2} \leq z \leq \frac{L}{2} \\
 H_y^{(III)}(x, z) &= \sqrt{\frac{\epsilon_0}{\mu_0}} \int_{-\infty}^{\infty} dk \tau(k) e^{ikx + i\sqrt{k_0^2 - k^2}(z - L/2)}, \quad \frac{L}{2} \leq z
 \end{aligned}$$

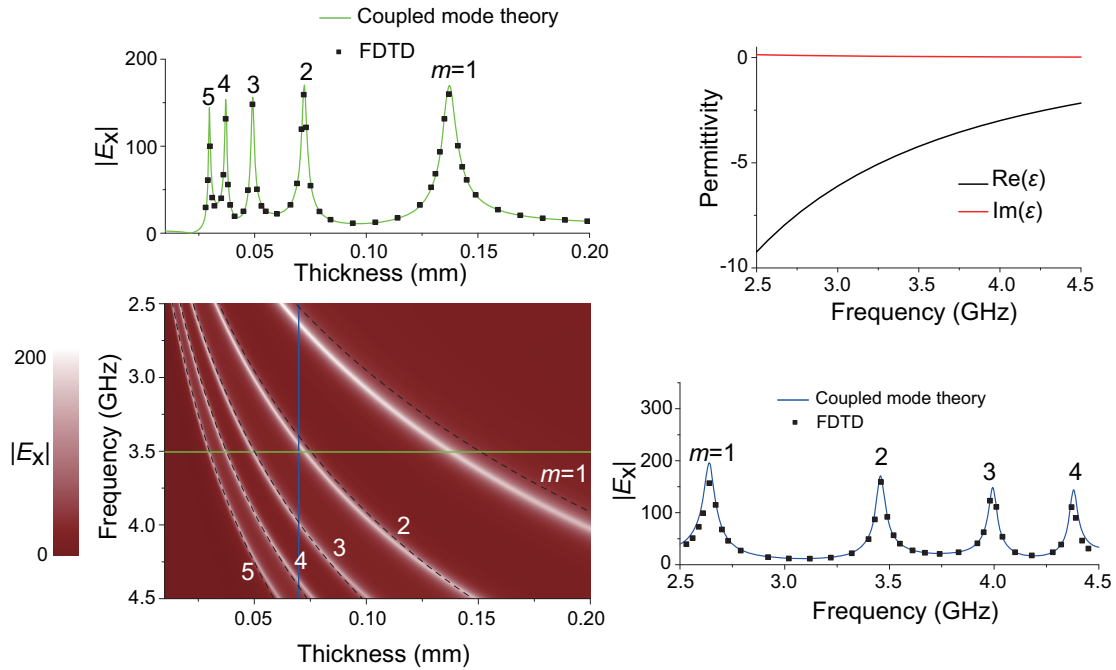


Figure 2 | Resonance characteristics of a vortex plasmon. Coupled-mode theory calculation of electric field amplitude plotted varying the frequency and slit waveguide length for a Drude-type dispersive filling medium with permittivity $\varepsilon(\omega) = 1 - \omega_p^2/(\omega^2 + i\gamma\omega)$, where $\omega_p = 16\pi$ GHz and $\gamma = 0.211$ GHz. A horizontal crosscut at a fixed frequency shows fractional behaviour, whereas a vertical crosscut at a fixed thickness produces spectral behaviour of vortex plasmon modes. All these theoretical predictions based on coupled mode theory agree nicely with the rigorous FDTD numerical results (filled squares). We set the slit width $a = 2$ mm and approximated the coupled mode theory by keeping the waveguide modes up to $m = 5$. Electric field amplitudes are the magnitude of the x component of the electric field calculated at the centre of the slit ($x = a/2, z = L/2$) by taking the incident field as the unit strength. This specific field component and measurement position were chosen because they conveniently describe vortex plasmon resonances.

where ε_0, μ_0 are the vacuum permittivity and permeability, respectively, $k_0 = 2\pi/\lambda$ is the wave number, $u_m(x) \equiv \cos(2m\pi x/a)$ $\sqrt{(2 - \delta_{m0})/a}$ are normalized slit mode functions, and $\theta_m \equiv \sqrt{\varepsilon k_0^2 - (2m\pi/a)^2}$ correspond to the longitudinal momenta. By requiring the continuity of the tangential magnetic field component H_y at the interface, $z = \pm L/2$, we obtain

$$A_m e^{-i\theta_m L/2} + B_m e^{i\theta_m L/2} = \int_{-\infty}^{\infty} dk (\delta(k) + \rho(k)) \int_0^a dx u_m(x) e^{ikx} \quad (2)$$

$$A_m e^{i\theta_m L/2} + B_m e^{-i\theta_m L/2} = \int_{-\infty}^{\infty} dk \tau(k) \int_0^a dx u_m(x) e^{ikx},$$

where we used the orthogonality of modes $u_m(x)$. Likewise, the continuity of the tangential electric field component E_x yields after the inverse Fourier transformation,

$$\sqrt{k_0^2 - k^2} (\delta(k) - \rho(k)) = \frac{1}{\varepsilon} \sum_{m=0}^{\infty} \left[\theta_m \left(A_m e^{-i\theta_m L/2} - B_m e^{i\theta_m L/2} \right) \frac{1}{2\pi} \int_0^a dx u_m(x) e^{-ikx} \right] \quad (3)$$

$$\sqrt{k_0^2 - k^2} \tau(k) = \frac{1}{\varepsilon} \sum_{m=0}^{\infty} \left[\theta_m \left(A_m e^{i\theta_m L/2} - B_m e^{-i\theta_m L/2} \right) \frac{1}{2\pi} \int_0^a dx u_m(x) e^{-ikx} \right]$$

Combining (2) and (3), one can readily obtain a matrix equation for unknown coefficients A_m and B_m in the form $MC = E$ with the matrix components given by

$$M_{2m+1, 2n+1} = M_{2m+2, 2n+2} = e^{-i\theta_n L/2} (\delta_{mn} + Z_{mn}),$$

$$M_{2m+1, 2n+2} = M_{2m+2, 2n+1} = e^{i\theta_n L/2} (\delta_{mn} - Z_{mn}) \quad (4)$$

$$C_{2m+1} = A_m, \quad C_{2m+2} = B_m,$$

$$E_{2m+1} = 2\sqrt{a} \delta_{m0}, \quad E_{2m+2} = 0, \quad (m, n = 0, 1, 2, \dots)$$

where Z_{mn} is the mode coupling constant,

$$Z_{mn} \equiv \frac{\theta_n}{2\pi\varepsilon} \int_0^a dx u_m(x) \int_0^a dy u_n(y) \int_{-\infty}^{\infty} dk \frac{e^{ik(x-y)}}{\sqrt{k_0^2 - k^2}} \quad (5)$$

$$= \frac{\theta_n}{2\varepsilon} \int_0^a dx u_m(x) \int_0^a dy u_n(y) H_0^{(1)}(k_0|x-y|),$$

and $H_0^{(1)}$ is the Hankel function of the first kind. Truncating the infinite-dimensional matrix equation to a finite-dimensional one of order N , we may solve the matrix equation approximately for coefficients A_m and B_m and subsequently obtain $\rho(k)$ and $\tau(k)$ from (3).

Because the mode coefficients A_m and B_m are obtained from the matrix inversion $C = M^{-1}E$, their maximum values arise around the minimum of the determinant of matrix M . Matrix M is dominated by 2×2 block diagonal elements, so the leading-order approximation of the determinant of M becomes the product of the determinants of 2×2 matrices $Q^{(mm)}$ such that

$$\det(M) \approx \prod_{m=0}^{\infty} \det(Q^{(mm)}) \quad (6)$$

$$= \prod_{m=0}^{\infty} [-(Z_{mm} - 1)^2 e^{i\theta_m L} + (Z_{mm} + 1)^2 e^{-i\theta_m L}].$$

In particular, the m -th-order resonance is obtained by minimizing the absolute value of the determinant of $Q^{(mm)}$, which becomes

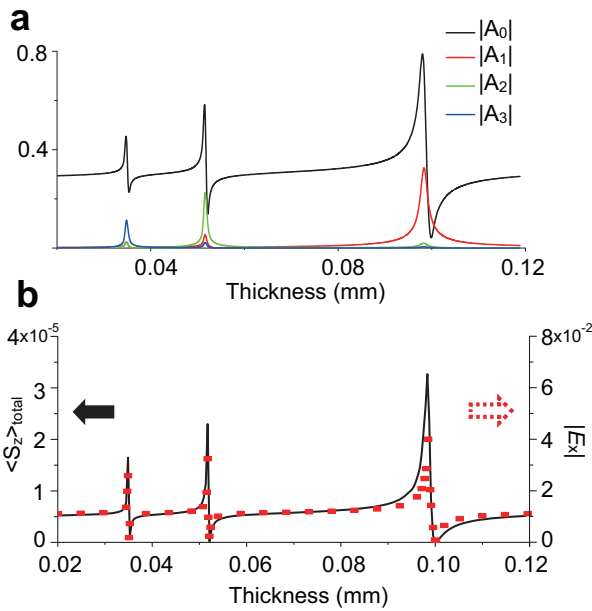


Figure 3 | FTR theory. (a) Coupling coefficients A_m of waveguide modes are plotted varying the thickness L . At the m -th order fractional tunnelling resonance, coefficients A_0 and A_m become resonantly excited. (b) The time averaged energy flux passing through the slit is plotted varying the thickness L . It shows nearly the same resonance behaviour as A_0 . Here, we set the frequency of incident to 3.0 GHz, slit width to 1 mm, and ϵ to $-3 + 0.001i$. Red square dots represent the magnitude of a local electric field E_x in the far-field region. Both the time averaged energy flux, i.e. transmission, and the far-field E_x exhibits the same resonance features according to the optical theorem.

$$\tanh(|\theta_m|L) = -\frac{2\text{Re}(Z_{mm})}{1 + |Z_{mm}|^2}. \quad (7)$$

For a narrow slit ($a < \lambda$), we find that $Z_{mm} \approx 2Si(2m\pi)/(\pi\epsilon)$, where $Si(x) \equiv \int_0^x dt \sin(t)/t$ and $\theta_m \approx i2m\pi/a$. Consequently, the resonance condition can be written as

$$L \approx L_m = \frac{a}{2m\pi} \ln \left| \frac{\epsilon\pi - 2Si(2m\pi)}{\epsilon\pi + 2Si(2m\pi)} \right|, m \geq 1 \quad (8)$$

This condition fails if $\epsilon > 0$. For $\epsilon < 0$, we have

$$L_m \approx \frac{a}{2m\pi} \ln \left| \frac{\epsilon - 1 + \frac{1}{m\pi^2}}{\epsilon + 1 - \frac{1}{m\pi^2}} \right| \approx \frac{a}{m\pi|\epsilon|}, \text{ for } \epsilon < -1 \text{ and } m \geq 1. \quad (9)$$

Thus, resonance arises at each fraction length L_m if the medium possesses negative permittivity, where the integer m corresponds to the m -th order waveguide mode. The m -th-order resonance arises from the excitation of a vortex plasmon, which is a coupled state between an m -th-order waveguide mode, in the form of a standing anti-symmetric slab plasmon, and an incident plane wave, as depicted in Fig. 1d (see the details on vortex plasmons in the Supplementary Information). The coupling between the incident wave and the slab plasmon creates channels for the circulating energy flow, thereby forming optical vortex-antivortex pairs. FTR arises from a resonant buildup of energy in the vortex plasmons, whereas the fractional behaviour results from the $1/m$ -dependence of the skin depth corresponding to the m -th order evanescent waveguide mode.

Figure 2 shows theoretical predictions of vortex plasmon resonance obtained by the analytic coupled mode theory as well as the rigorous numerical FDTD calculation. Because materials possessing negative permittivity are generally dispersive, and the fractional lengths L_m are inversely proportional to the permittivity, vortex plasmon resonance in a Drude-type dispersive material manifests

itself as the spectral resonance. This is shown clearly in Fig. 2 where enhanced local electric fields are plotted as a function of the thickness L and frequency f . Curved dashed lines indicate the approximate resonance conditions in (9), which show good agreement with the full calculation of the coupled mode theory. Crosscuts obtained by fixing L or f at specific values are drawn separately in Fig. 2. The crosscut obtained at a constant f as a function of thickness clearly shows the fractional nature of the resonance, whereas that obtained at a fixed L as a function of frequency shows a resonance spectrum of vortex plasmons. Both crosscuts agree nicely with rigorous numerical results obtained using the FDTD method.

So far, we have discussed the resonance of locally excited vortex plasmons. To understand the resonant tunnelling behaviour, we consider the transmission of light into the far-field, which is given by the time-averaged total energy flux through the slit:

$$\langle S_z \rangle_{total} \equiv \frac{1}{2} \int_0^a dx \text{Re}(E_x H_y^*) \quad (10)$$

Assuming $\epsilon < 0$ and using the Maxwell's equation to obtain E_x from (1), we may write

$$\langle S_z \rangle_{total} = i \frac{1}{\epsilon} \sqrt{\frac{\epsilon_0}{\mu_0}} \sum_{m=0}^{\infty} \left[\frac{\theta_m}{k_0} \text{Im}(A_m B_m^*) \right] \approx \frac{1}{|\sqrt{\epsilon}|} \sqrt{\frac{\epsilon_0}{\mu_0}} \text{Im}(A_0 B_0^*) \quad (11)$$

where the approximation in the last step holds since $A_m \approx -B_m$ ($m \geq 1$) in the configuration of vortex plasmons (see the Supplementary Information).

In Fig. 3, magnitudes $|A_m|$ and transmission $\langle S_z \rangle_{total}$ are plotted varying the thickness L . Note that, at the m -th order resonance in Fig. 3a, the mode coefficients (A_0, B_0) and (A_m, B_m) are dominantly excited due to the excitation of the m -th order vortex plasmon which reflects the fact that the vortex plasmon is a coupled state between the m -th order slab plasmon and the incident wave. It should be noted that transmission is also governed by A_0 as in (11). In Fig. 3b, the full calculation of transmission without approximation shows nearly the same resonance behaviour as A_0 . Subsequently, resonant light tunnelling also occurs at fractional lengths, thereby justifying the name *fractional tunnelling resonance* (FTR).

Experimental verification. To confirm FTR and the occurrence of vortex plasmons experimentally, we performed a microwave measurement using the experimental setup shown in Fig. 4a. With a hairpin monopole antenna, we measured the local electric field components near a slit 65 mm wide in an aluminium plate 2.4 mm thick. The slit was filled with a negative permittivity medium; we used a metamaterial made of staples embedded in a Styrofoam™ board, as specified in Fig. 4b. The staples were arranged in a periodic split rectangle pattern inside a Styrofoam™ board that possessed an air-like permittivity ($\epsilon \approx 1.03$). This metamaterial was chosen because it exhibits almost lossless behaviour at microwave frequencies of 2.6–3.9 GHz. The permittivity in this frequency range possesses a relatively small negative real part and a negligible imaginary part, as shown in Fig. 4c, and the material's spectral behaviour is fitted well by the Drude model. These features of the permittivity make it easy to measure the FTR and vortex plasmon modes with a relatively thick fractional thickness L_m and sharper resonance peaks.

Figure 5 shows a spectral map of the measured electric near fields, where the vertical crosscut describes a vortex plasmon mode across the slit at a fixed frequency. Vortex plasmons are excited by normally incident light polarized perpendicular to the slit direction (only the electric field component E_x is nonzero). The x component of the local electric field was measured using a hairpin monopole antenna across the slit at a distance of 5 mm from the aluminium plate. The local enhancement factor, defined as the ratio between the local electric field and the incident field, is expressed in a two-dimensional plot with spatial mode profiles on the vertical axis and frequencies on the

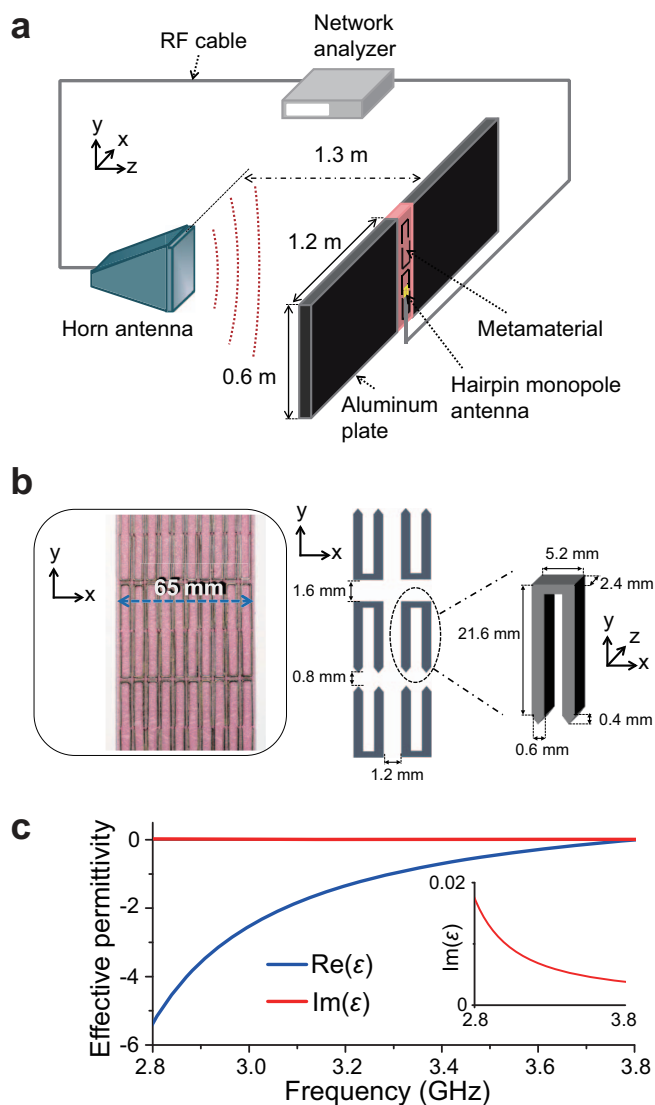


Figure 4 | Experimental setup. (a) Schematics of microwave measurement system. (b) Photo of the metamaterial used or a filling medium (left) consisting of staples embedded in a Styrofoam™ board. Detailed specifications of U-shaped staples and alignments (right). (c) Effective permittivity of the metamaterial sample. Permittivity was obtained from the calculated transmission and reflection coefficients using the FDTD method.

horizontal axis. The experimentally measured enhancement factor is given in Fig. 5a and agrees well with the FDTD numerical result in Fig. 5b. The horizontal cut (blue dashed line) represents the spectrum of a local electric field at the centre of the slit. It clearly shows resonant spectral peaks corresponding to the first four vortex plasmon modes ($m = 1, 2, 3, 4$). Vertical cuts also show the $2m + 1$ nodes of the m -th-order vortex plasmon. These results may be compared with the theoretically calculated spectral map in Fig. 5c for the homogeneous case, where we assumed that the slit was filled with a homogeneous material possessing the effective permittivity of the metamaterial described above.

In order to confirm FTR experimentally, we conducted a far-field measurement of local E_x field which faithfully reproduces transmission resonances as described in Fig. 3b. This agreement arises from the optical theorem²⁷ which relates the transmission as a total scattering cross-section to the forward-scattered field. By using a 20-millimeter-long straight monopole antenna, E_x field was measured at the location 100 mm away from the centre of metamaterial filled

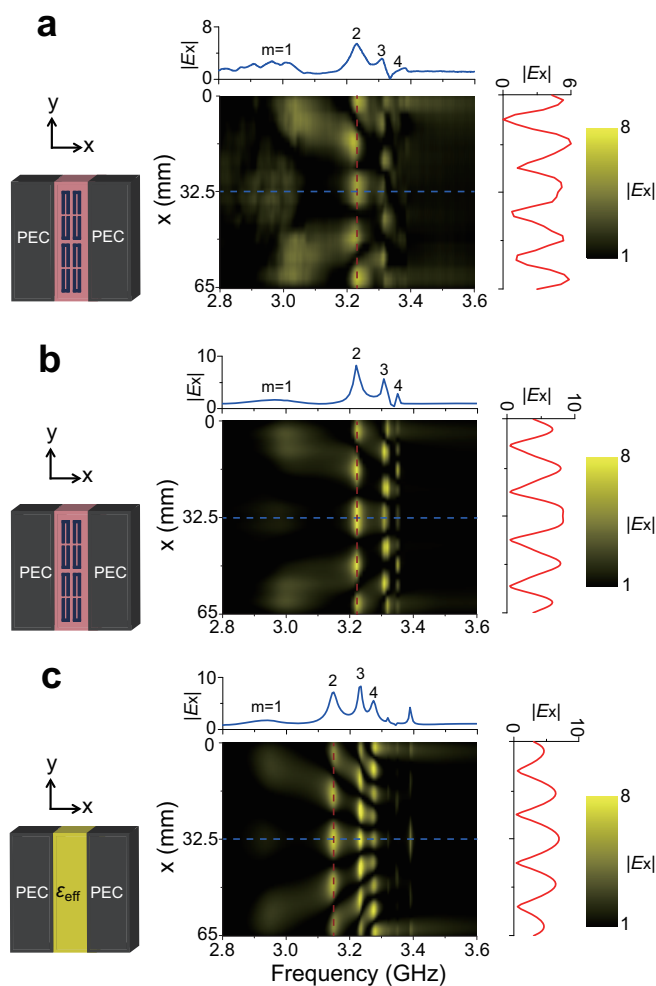


Figure 5 | Spectral map of vortex plasmon modes. (a) Experimentally measured vortex plasmon modes. Local electric field amplitude $|E_x|$ across the metamaterial-filled slit region was measured by moving a hairpin monopole antenna across the slit at a distance of 5 mm from the aluminium plate. Horizontal crosscut at the centre of a slit shows the first three spectral peaks corresponding to vortex plasmon modes, whereas the vertical cut shows the mode profile for the $m = 2$ mode. (b) FDTD numerical results for the same system. (c) Analytically calculated spectral map assuming that the slit-filling medium is a homogeneous material having the effective permittivity shown in Fig. 4c.

slit. Figure 6 shows experimentally measured and numerically calculated FTRs. In Fig. 6a, experimentally measured far-field transmission resonances are compared with resonances of near-field vortex plasmons. The first three FTR peaks ($m = 1, 2, 3$) are clearly shown and they exhibit a good agreement with the FDTD numerical results shown in Fig. 6b. Analytically calculated FTR from the slit filled with a homogeneous negative permittivity material is given in Fig. 6c, which also show a good qualitative agreement with the metamaterial case.

Discussion

We note that the finite size of a staple in the metamaterial limits the spatial resolution required for higher vortex plasmon modes and FTR, and shifts the resonance peaks compared to the homogeneous case. Despite the limited spatial resolution, it is remarkable that our metamaterial sample faithfully resolves the first four vortex plasmon modes and three FTR peaks, which also appear for the homogeneous material. The fourth-order FTR peak is barely visible in the experimental measurement because of background noise.

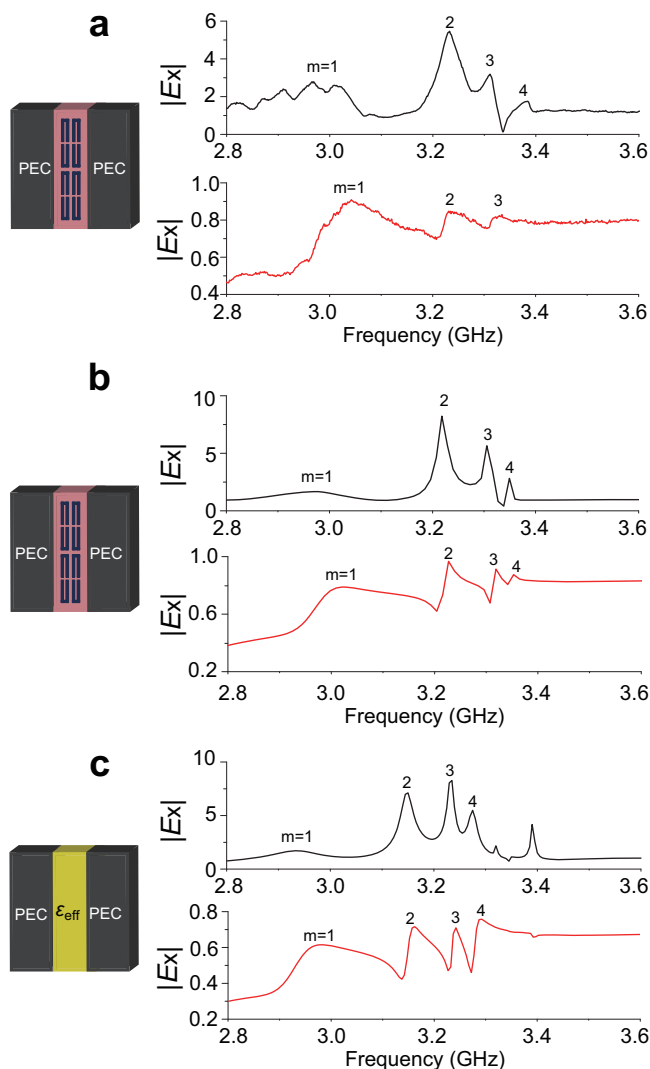


Figure 6 | FTR spectrum. (a) Experimentally measured FTR spectrum. Local field amplitude E_x in the far-field region was measured at a location 100 mm apart from the slit (bottom). Near-field vortex plasmon spectrum is also shown for comparison (top) (b) FDTD numerical results for the same system. (c) Coupled mode theory calculation of FTR spectrum (bottom) for the slit filled with homogeneous material possessing the effective permittivity given in Fig. 4c.

Excitation of vortex plasmon modes strongly enhances the local electric field, by a factor of 150 in Fig. 2 and 10 in Fig. 5, where a narrower slit exhibits a stronger enhancement due to the capacitive coupling of light to the slit^{28,29}.

In conclusion, we have shown that resonant tunnelling can arise in fractionally thin metals. We have also demonstrated fractional tunnelling resonance and vortex plasmons experimentally in the microwave regime using metamaterials. Fractional tunnelling resonance can be directly applied to the communication antenna technology³⁰ and the strong amplification of local electromagnetic fields^{28,29,31}. Fractional tunnelling resonance provides a new paradigm for the ultra-thin metal resonator.

Methods

To confirm the vortex plasmon modes and FTR experimentally, we prepared a microwave near and far-field measurement system as shown in Fig. 4a. We prepared two $1.2 \text{ m} \times 0.6 \text{ m}$ aluminium plates, which stood separated by a gap of 65 mm to form a $65 \text{ mm} \times 0.6 \text{ m}$ slit. A Hewlett-Packard 8719C network analyser and SGH 260 standard gain horn antenna were used to generate and detect the x -polarized pulse of an electric field covering the spectral range between 2.6 GHz and 3.9 GHz. A hairpin monopole antenna was used to detect the local electric field component E_x near the

sample, and 20-millimeter-long straight monopole antenna was used to measure E_x in far-field. Metamaterials were made by embedding U-shaped galvanized iron staples periodically in a Styrofoam™ board (see the Supplementary Information for details). The effective permittivity and permeability of a material were determined by measuring the transmission and reflection coefficients and using the Nicolson–Ross–Weir method. For the numerical calculations, we used the finite-difference time-domain method with a grid size of 0.05 mm. The dispersive materials were modelled as Drude dispersive media and handled using the auxiliary differential equation method.

- Little, B. E. *et al.* Ultra-compact Si-SiO microring resonator. *IEEE Photon. Tech. Lett.* **10**, 549–551 (1998).
- Xia, F., Sekaric, L. & Vlasov, Y. Ultracompact optical buffers on a silicon chip. *Nature Photon.* **1**, 65–71 (2007).
- Armani, A. M., Kulkarni, R. P., Fraser, S. E., Flagan, R. C. & Vahala, K. J. Label-free, single-molecule detection with optical microcavities. *Science* **317**, 783–787 (2007).
- Anker, J. N., Hall, W. P., Lyanders, O., Shah, N. C., Zhao, J. & Duyne, R. P. V. Biosensing with plasmonic nanosensors. *Nature Mat.* **7**, 8–10 (2008).
- Cattoni, A. *et al.* $\lambda^3/1000$ Plasmonic nanocavities for biosensing fabricated by soft UV nanoimprint lithography. *Nano Lett.* **11**, 3557–3563 (2011).
- Michler, P. *et al.* A quantum dot single-photon turnstile device. *Science* **290**, 2282–2285 (2000).
- Choy, J. T. *et al.* Enhanced single-photon emission from a diamond-silver aperture. *Nature Photon.* **5**, 738–743 (2011).
- Sandoghdar, V. *et al.* Very low threshold whispering-gallery-mode microsphere laser. *Phys. Rev. A* **54**, R1777–R1780 (1996).
- Colombelli, R. *et al.* Quantum cascade surface-emitting photonic crystal laser. *Science* **302**, 1374–1377 (2003).
- Hill, M. T. *et al.* Lasing in metallic-coated nanocavities. *Nature Photon.* **1**, 589–594 (2007).
- Oulton, R. F. *et al.* Plasmon lasers at deep subwavelength scale. *Nature* **461**, 629–632 (2009).
- Nezhad, M. P. *et al.* Room-temperature subwavelength metallo-dielectric lasers. *Nature Photon.* **4**, 395–399 (2010).
- Shalaev, V. M. Optical negative-index metamaterials. *Nature Photon.* **1**, 41–48 (2007).
- Soukoulis, C. M. & Wegener, M. Past achievements and future challenges in the development of three-dimensional photonic metamaterials. *Nature Photon.* **5**, 523–530 (2011).
- Atwater, H. A. & Polman, A. Plasmonics for improved photovoltaic devices. *Nature Mat.* **9**, 205–213 (2010).
- Bohm, D. *Quantum Theory* (Prentice-Hall, Englewood Cliffs, New Jersey, 1951).
- Zhou, L., Wen, W., Chan, C. T. & Sheng, P. Electromagnetic-wave tunneling through negative-permittivity media with high magnetic fields. *Phys. Rev. Lett.* **94**, 243905 (2005).
- Hooper, I. R., Preist, T. W. & Sambles, J. R. Making tunnel barriers (including metals) transparent. *Phys. Rev. Lett.* **97**, 053902 (2006).
- Ebbesen, T. W., Lezec, H. J., Ghaemi, H. F., Thio, T. & Wolff, P. A. Extraordinary optical transmission through sub-wavelength hole arrays. *Nature* **391**, 667–669 (1998).
- Ruan, Z. & Qiu, M. Enhanced transmission through periodic arrays of subwavelength holes: the role of localized waveguide resonance. *Phys. Rev. Lett.* **96**, 233901 (2001).
- Martín-Moreno, L. *et al.* Theory of extra ordinary optical transmission through subwavelength hole arrays. *Phys. Rev. Lett.* **86**, 1114–1117 (2001).
- Fan, R. H. *et al.* Transparent metals for ultrabroadband electromagnetic waves. *Adv. Mater.* **24**, 1980–1986 (2012).
- Aliù, A., D’Aguanno, G., Mattiucci, N. & Bloemer, M. J. Plasmonic Brewster Angle: Broadband extraordinary transmission through optical gratings. *Phys. Rev. Lett.* **106**, 123902 (2011).
- Aydin, K. *et al.* Splint-ring-resonator-coupled enhanced transmission through a single subwavelength aperture. *Phys. Rev. Lett.* **102**, 013904 (2009).
- Kang, J. H., Choe, J.-H., Kim, D. S. & Park, Q.-H. Substrate effect on aperture resonance in a thin metal film. *Opt. Express* **17**, 15652–15658 (2009).
- Petit, R. *Electromagnetic theory of gratings* (Springer-Verlag, Berlin, 1980).
- Jackson, J. D. *Classical electrodynamics* (Wiley: New York, 1999).
- Seo, M. A. *et al.* Terahertz field enhancement by a metallic nano slit operating beyond the skin-depth limit. *Nature Photon.* **3**, 152–156 (2009).
- Kang, J. H., Kim, D. S. & Park, Q.-H. Local capacitor model for plasmonic electric field enhancement. *Phys. Rev. Lett.* **102**, 093906 (2009).
- Balanis, C. A. *Antenna theory* (Wiley, New York, 2005).
- Park, Q.-H. Optical antennas and plasmonics. *Cont. Phys.* **50**, 407–423 (2009).

Acknowledgements

We thank Dong-Hyun Cho, Dai-Sik Kim and Jong-Ho Choe for discussion. This work was supported by the National Research Foundation of Korea (NRF) grant funded by the Korea government (MEST) (No.2012-0008686) and the Green Nano Technology Development Program (2012-0006655).



Author contributions

Q.-H.P. developed the theory and J.-H.K. performed the microwave measurement and the numerical calculation. Q.-H.P. and J.-H.K. analyzed the data and wrote the manuscript.

Additional information

Supplementary information accompanies this paper at <http://www.nature.com/scientificreports>

Competing financial interests: The authors declare no competing financial interests.

How to cite this article: Kang, J.-H. & Park, Q.-H. Fractional tunnelling resonance in plasmonic media. *Sci. Rep.* 3, 2423; DOI:10.1038/srep02423 (2013).



This work is licensed under a Creative Commons Attribution-NonCommercial-NoDerivs 3.0 Unported license. To view a copy of this license, visit <http://creativecommons.org/licenses/by-nc-nd/3.0>